Original Article | Thoracic Imaging

https://doi.org/10.3348/kjr.2016.17.6.950
pISSN 1229-6929 · eISSN 2005-8330
Korean J Radiol 2016;17(6):950-960

Korean Journal of Radiology
KJR

The Impact of Iterative Reconstruction in Low-Dose Computed Tomography on the Evaluation of Diffuse Interstitial Lung Disease

Hyun-ju Lim, MD, Myung Jin Chung, MD, Kyung Eun Shin, MD, Hye Sun Hwang, MD, Kyung Soo Lee, MD

All authors: Department of Radiology and Center for Imaging Science, Samsung Medical Center, Sungkyunkwan University School of Medicine, Seoul 06351, Korea

Objective: To evaluate the impact of iterative reconstruction (IR) on the assessment of diffuse interstitial lung disease (DILD) using CT.

Materials and Methods: An American College of Radiology (ACR) phantom (module 4 to assess spatial resolution) was scanned with 10–100 effective mAs at 120 kVp. The images were reconstructed using filtered back projection (FBP), adaptive statistical iterative reconstruction (ASIR), with blending ratios of 0%, 30%, 70% and 100%, and model-based iterative reconstruction (MBIR), and their spatial resolution was objectively assessed by the line pair structure method. The patient study was based on retrospective interpretation of prospectively acquired data, and it was approved by the institutional review board. Chest CT scans of 23 patients (mean age 64 years) were performed at 120 kVp using 1) standard dose protocol applying 142–275 mA with dose modulation (high-resolution computed tomography [HRCT]) and 2) low-dose protocol applying 20 mA (low dose CT, LDCT). HRCT images were reconstructed with FBP, and LDCT images were reconstructed using FBP, ASIR, and MBIR. Matching images were randomized and independently reviewed by chest radiologists. Subjective assessment of disease presence and radiological diagnosis was made on a 10-point scale. In addition, semi-quantitative results were compared for the extent of abnormalities estimated to the nearest 5% of parenchymal involvement.

Results: In the phantom study, ASIR was comparable to FBP in terms of spatial resolution. However, for MBIR, the spatial resolution was greatly decreased under 10 mA. In the patient study, the detection of the presence of disease was not significantly different. The values for area under the curve for detection of DILD by HRCT, FBP, ASIR, and MBIR were as follows: 0.978, 0.979, 0.972, and 0.963. LDCT images reconstructed with FBP, ASIR, and MBIR tended to underestimate reticular or honeycombing opacities (-2.8%, -4.1%, and -5.3%, respectively) and overestimate ground glass opacities (+4.6%, +8.9%, and +8.5%, respectively) compared to the HRCT images. However, the reconstruction methods did not differ with respect to radiologic diagnosis.

Conclusion: The diagnostic performance of LDCT with MBIR was similar to that of HRCT in typical DILD cases. However, caution should be exercised when comparing disease extent, especially in follow-up studies with IR.

Keywords: *Model-based iterative reconstruction; Adaptive statistical iterative reconstruction; Computed tomography; Spatial resolution; Interstitial lung disease*

Received August 29, 2015; accepted after revision July 28, 2016.
Presented in abstract form at the Annual Meeting of the Radiological Society of North America 2013 in Chicago, IL.
Corresponding author: Myung Jin Chung, MD, Department of Radiology and Center for Imaging Science, Samsung Medical Center, Sungkyunkwan University School of Medicine, 81 Irwon-ro, Gangnam-gu, Seoul 06351, Korea.
• Tel: (822) 3410-2519 • Fax: (822) 3410-2525 • E-mail: mj1.chung@samsung.com

Korean Journal of Radiology
KJR

INTRODUCTION

With the growing use of computed tomography (CT), the increase in the medical radiation exposure has recently become a problem. Especially, the cumulative radiation burden is a particular concern for patients who require serial follow-up CT scans, including patients with idiopathic interstitial pneumonias (IIPs). There have been considerable modifications to CT protocols over the last decade in an attempt to reduce radiation exposure (1-3). For example, use of tube current modulation (4), reduced tube voltage (5), higher pitch (6) and noise reduction filters (7) has been shown to reduce radiation exposure. However, there is a trade-off between image quality and radiation dose. Therefore, iterative reconstruction (IR) has recently been reintroduced as a method to improve CT image quality, enhance resolution, and reduce noise.

One of the first generation IR algorithms released for clinical use was the adaptive statistical iterative reconstruction (ASIR) (GE Healthcare, Waukesha, WI, USA). By modelling photon and electronic noise statistics, ASIR reduces image quantum noise without compromising spatial or contrast resolution through a more complex analysis of detector response and statistical behavior of CT measurements compared with the conventional filtered back projection (FBP) algorithm (8). Most IR algorithms including ASIR are called hybrid IR because they are not fully iterative but are used in combination with FBP. A much more advanced algorithm approaching true IR was developed recently and it is called model-based iterative reconstruction (MBIR). It uses backward and forward projections to iteratively match the reconstructed image to the acquired data based on a statistical metric. MBIR models simulate not only system statics (as in ASIR), but also system optics. Thus, important physical factors such as focal spot and detector geometry, photon statistics, X-ray beam spectra, and scattering are more accurate compared to those of FBP. While the MBIR technique requires more time for reconstruction, the images were reported to exhibit substantially less noise than ASIR or FBP images (9, 10).

Image noise and spatial resolution greatly affect CT image quality (11, 12). As details of the pulmonary interstitium like reticular opacities require high spatial resolution for evaluation in patients with diffuse interstitial lung disease (DILD), it is presumed that loss of spatial resolution under a low dose setting might interfere with the initial disease diagnosis or comparison of disease extent on follow-up. However, previous studies on the effect of IR on lung parenchymal lesions (13-16) did not focus on radiological diagnosis and disease extent evaluation in conventional IIPs including usual interstitial pneumonia (UIP), nonspecific interstitial pneumonia (NSIP) and cryptogenic organizing pneumonia (COP). Therefore, a practical concern was raised that the use of IR might affect the perceived extent of DILD lesions in which high spatial resolution is essential and may have an impact on patient management.

The aim of this study was to evaluate the effect of reconstruction methods including FBP, ASIR, and MBIR on the assessment of DILD using CT.

MATERIALS AND METHODS

Phantom and Objective Measurements

We used the American College of Radiology CT phantom (Gammex 464, Gammex Inc., Middleton, WI, USA). Module 4, which is designed to assess high contrast (spatial) resolution, contained eight high contrast resolution patterns of 4, 5, 6, 7, 8, 9, 10 and 12 line pairs per cm and it was scanned with a 64-section multidetector row CT scanner (GE Discovery 750 HD; GE Healthcare, Milwaukee, WI, USA) with a tube voltage of 120 kVp, tube currents of 20 mA and 195 mA (10–100 effective mA/slice), a pitch of 0.969, and a rotation speed of 0.5 seconds. The scanned data from module 4 of the ACR CT phantom were reconstructed with FBP, ASIR, and MBIR reconstruction algorithms to assess high contrast (i.e., spatial) resolution. The blending ratios for ASIR were classified into the following five different levels: 0% (i.e., non-ASIR, which was equal to FBP), 30%, 50%, 70%, and 100%.

Instead of the modulation transfer function, spatial resolution was calculated using the line pair structure method (17) as suggested by Staude and Goebbels (17). The contrast was measured at a gray value profile along the line in the reconstructed volume, wherein the gray value minima ($N_A[i]$) were determined in the cut-outs and the maxima ($N_B(i)$) were determined in the material bridges (Fig. 1A, B). The contrast factor, R(i), is the difference between $N_B(i)$ and $N_A(i)$ and it was normalized to the gray value difference of the undisturbed material (N_A) and the undisturbed background (N_C), multiplied by 100:

$R(i) = (N_B[i]\text{-}N_A[i]/[N_C–N_A]) \times 100$

When the radiation dose and reconstruction method settings are held constant, the denominator ($N_C–N_A$) remains the same and the numerator ($N_B[i]–N_A[i]$) (expressed in

Hounsfield Unit [HU]) is directly proportional to R(i).

Patient Population

The institutional review board approved this retrospective study, and the requirment of informed consent was waived for the use of patient medical data. Patient consent was obtained for performing CT studies. A total of 23 consecutive patients were included between September 2012 and January 2013. CT scan was performed because of clinical or radiological suspicion of interstitial lung disease on the chest radiograph. All patients underwent routine protocol CT evaluation of interstitial lung disease, which included standard-dose thin-section non-helical high-resolution CT (HRCT), and helical low-dose CT (LDCT). We excluded the patients with severe emphysema, radiation pneumonitis, post-operative change or pneumonia.

Of the 23 subjects who were finally included in the current study, 13 were men and 10 were women, with a mean age of 64 ± 6 years. Five patients had no evidence of diffuse interstitial lung disease, and 18 patients had DILD. Among the 18 DILD patients, nine had UIP, three had fibrotic NSIP or less likely UIP, three had NSIP and three had COP. Most of the patients who had typical findings on CT were diagnosed radiologically by consensus among clinicians and were managed without pathological confirmation. However, 3 cases of UIP and 2 cases of COP were confirmed after surgical biopsy. Two other NSIP patients, in whom pathologic confirmation was not obtained, included patients with connective tissue disorders such as Sjögren's syndrome and systemic lupus erythematosus, respectively.

Computed Tomography Protocols and Image Reconstruction

Supine inspiratory HRCT scans of all patients were obtained without intravenous contrast using the same CT scanner. The protocols consisted of sections reconstructed with a high-spatial-frequency algorithm at 1- or 2-cm intervals under automatic exposure control (142–275 mA with dose modulation) with a slice thickness of 1.25 mm, from apex to base. We used a fixed tube current of 20 mAs per slice (40 mA with half second rotation and 0.984 pitch) for LDCT, which is appropriate according to the guideline of the Korean Society of Thoracic Radiology. Slice thickness of 1.25 mm and high-spatial-frequency algorithm were applied for LDCT.

This study used a tube current of 20 mAs per slice (40 mA with 0.5 second rotation and 0.984:1 beam pitch) for LDCT. For LDCT acquisition, the chest CT protocol used the helical mode with the following parameter: 1.25 mm x 64 detector configuration. Other scanning parameters were the same for HRCT and LDCT: peak tube voltage of 120 kVp, 40-mm table feed per gantry rotation, pitch of 0.984:1, and z-axis tube current modulation. The CT dose index volume ($CTDI_{vol}$) and dose-length product (DLP) were recorded for matched standard-dose HRCT and LDCT. A total of four series were obtained using the HRCT and LDCT images. The HRCT images were reconstructed using FBP (Series A). Three different reconstructions of the LDCT images were obtained: Series B with FBP (0% ASIR), Series C with 50% ASIR, and Series D with MBIR (Veo GE Healthcare, Milwaukee, WI, USA).

Subjective Evaluation for Patient Studies

Images at the levels of the aortic arch, left atrium, and lung bases were used. Matching images were randomly selected from the four series mentioned above (A-D). A total of 276 anonymized images (23 subjects x 3 levels x 4 series) were displayed in the lung window setting (width-1500 HU; level-700 HU) and were randomly aggregated into folders. Four board-certified chest radiologists independently reviewed the images while blinded to the tube current and method of image reconstruction.

In an effort to determine the confidence level of their diagnoses, radiologists were asked to rate their confidence using a continuous rating scale from 0 to 10. A score of 0 indicated that the abnormality was not present with absolute certainty, and a score of 10 indicated that the abnormality was present with absolute certainty. Ratings between 0 and 10 were interpreted as intermediate levels of confidence (1–4, "probably negative"; 5, "neutral"; 6–9, "probably positive"). If the observer's rating was greater than 6, the images fell into the category of "possible presence of interstitial lung disease."

Radiologists were also asked to estimate the overall extent of ground glass opacity, reticular opacity or honeycombing, and consolidation. The score was estimated to the nearest 5% of parenchymal involvement. Finally, radiologists categorized the disease based on a numerical scale. A score of 0 indicated that the abnormality resulted from COP or NSIP, and a score of 10 indicated a diagnosis of UIP. Ratings between 0 and 10 were interpreted as intermediate levels of confidence (1–4, probable COP or NSIP; 5, neutral; 6–9, probable UIP).

Korean Journal of Radiology
KJR

Statistical Analysis

A total of 1104 observations (23 subjects x 3 levels x 4 series x 4 observers) were subsequently evaluated. For the extent of diffuse interstitial lung abnormalities (i.e., ground glass opacity, reticular opacity or honeycombing, and consolidation), agreement between the extent determined

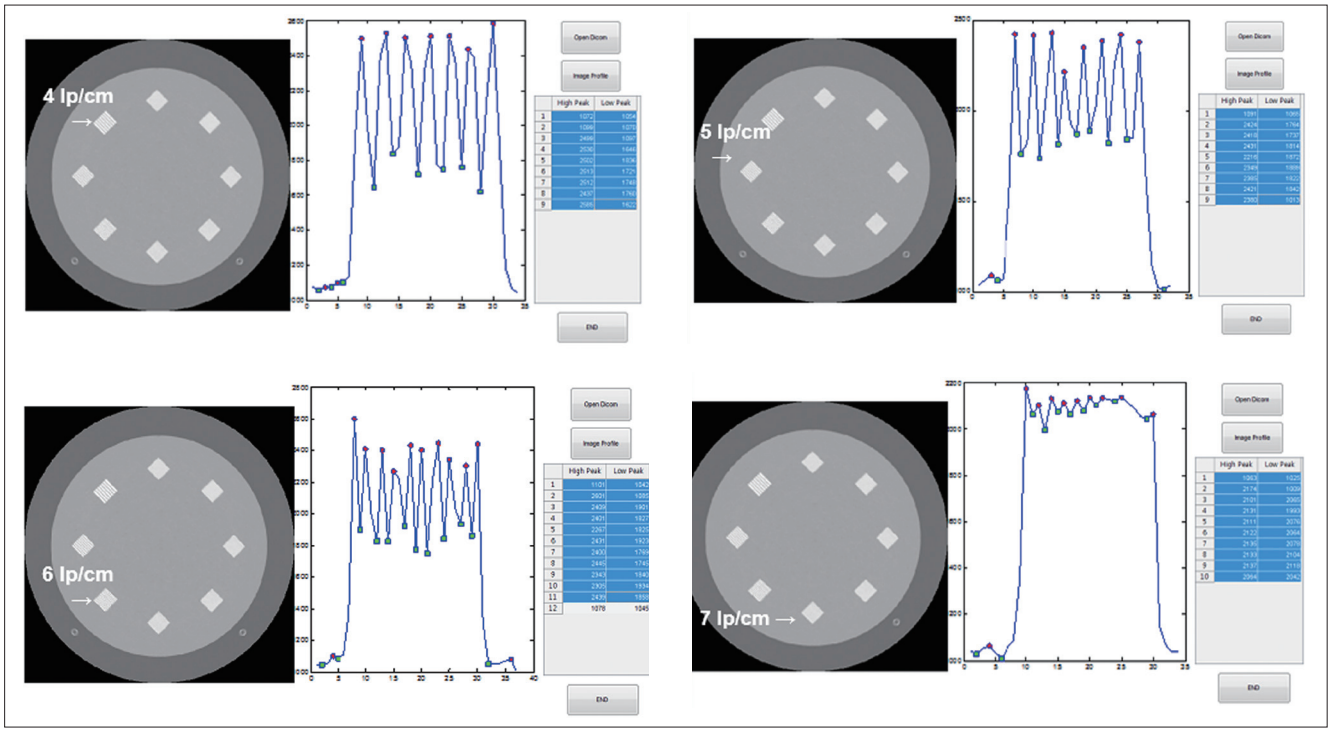

A

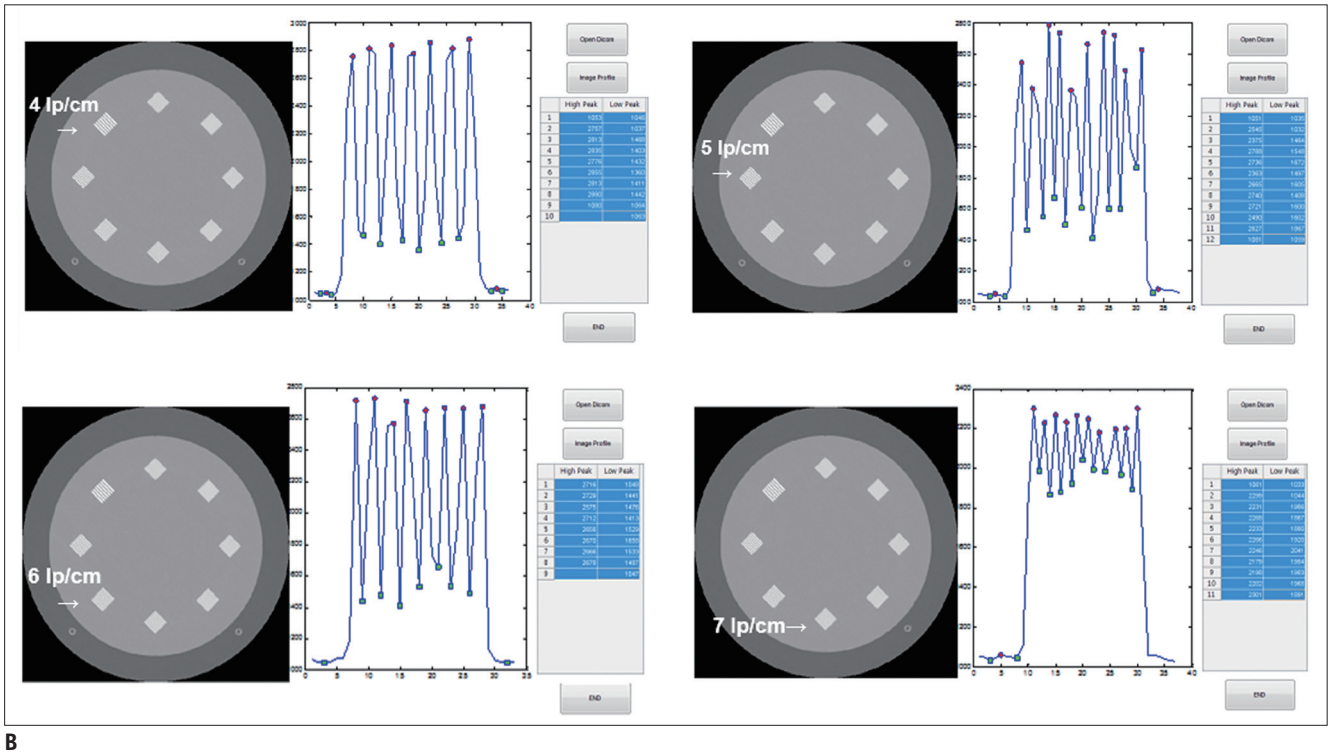

B

Fig. 1. Example results of phantom study with model-based iterative reconstruction (MBIR) are shown (A, scanned under 120 kVp, 10 mA); B (120 kVp, 50 mA). (A) shows significant decrease in difference between maximal and minimum values ($N_B[i]–N_A[i]$) in higher spatial resolution phantom images (7 lp/cm) at lower dose (120 kVp, 10 mA) compared with **(B)** (120 kVp, 50 mA).

using LDCT images with different reconstruction methods (i.e., FBP, ASIR, and MBIR) and that using standard-dose HRCT images was assessed using the Bland and Altman method. Bland Altman (18) plots were generated to compare differences in the estimations made using each reconstruction method. HRCT results were used as the reference standard.

The confidence levels for the presence of abnormalities and the radiological diagnosis of ILD on CT images using different reconstruction methods were recorded and subsequently analyzed using a receiver operating characteristic (ROC) technique. Area under the ROC curve (AUC) was used to indicate the overall performance of the observers for each data set and reconstruction modality (19, 20). Statistical analyses were performed using SPSS for Windows (version 17.0; SPSS Inc., Chicago, IL, USA), and *p* values < 0.05 were considered statistically significant.

RESULTS

Objective Measurements from the Phantom Study

Examples of numerator value measurements from MBIR images at 10 mA and 50 mA are shown in Figure 1A, B, respectively. The gray value minima $N_A(i)$ are expressed as green points, and the gray value maxima $N_B(i)$ are expressed as red points.

For relatively lower spatial resolution phantom images (4-6 lp/cm shown in Figure 1A, B), the differences between gray value minima and maxima were well preserved even for a lower radiation dose. However, the last graphs in Figure 1A (120 kVp, 10 mA) and Figure 1B (120 kVp, 50 mA) illustrate a significant decrease in the difference between maximal and minimal values (i.e., $N_B[i]–N_A[i]$) in the higher spatial resolution phantom images (7 lp/cm) at both radiation doses.

Under the same radiation dose and method of reconstruction (listed in Table 1), the denominator of the equation ($N_C–N_A$) should be the same. Therefore, the numerator, $N_B(i)–N_A(i)$, is directly correlated with the amount of contrast factor, R(i), when using the same radiation dose and reconstruction method. Figure 1C reveals the changes in the numerator (i.e., $N_B[i]–N_A[i]$) value in relation to spatial resolution. When compared to images reconstructed with FBP and ASIR, MBIR resulted in a relatively significant decrease in the numerator values at 10 mA for the bar resolution pattern with 7 lp/cm.

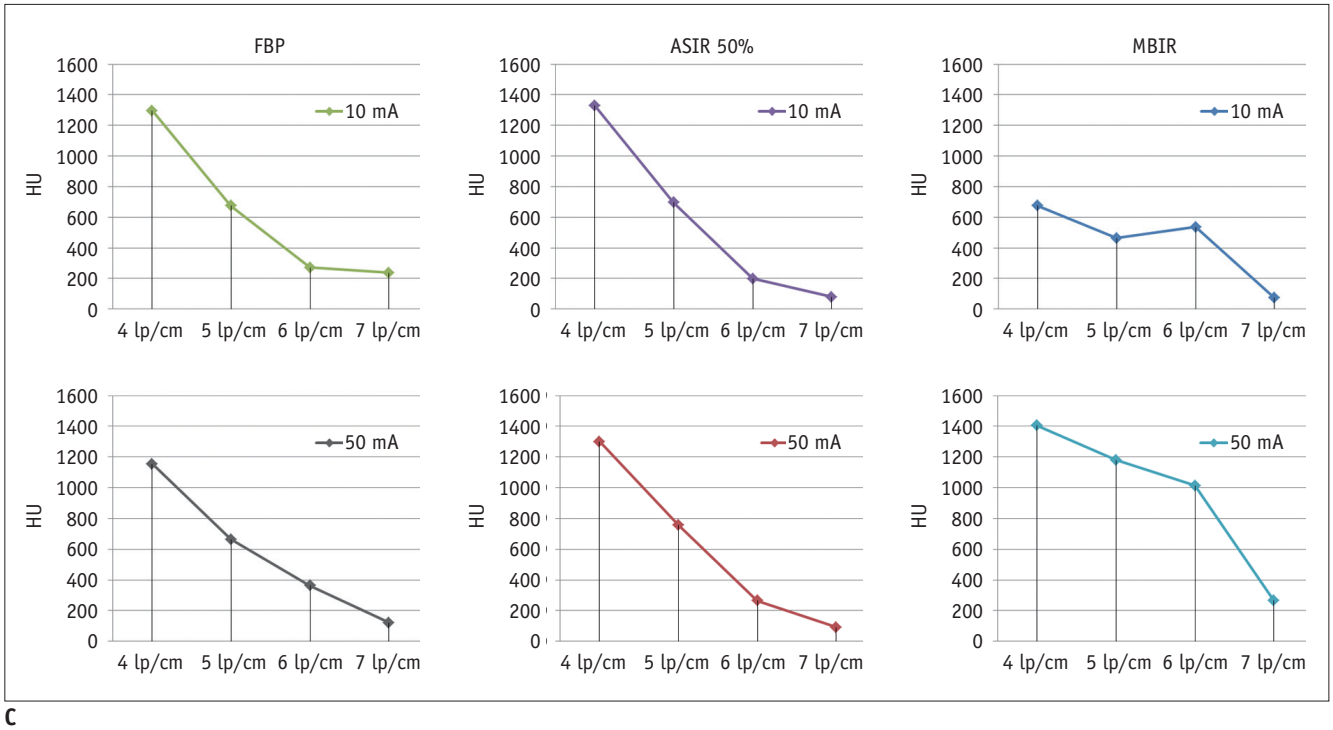

C

Fig. 1. Example results of phantom study with model-based iterative reconstruction (MBIR) are shown (A, scanned under 120 kVp, 10 mA); B (120 kVp, 50 mA). (C) shows changes in numerator value when using same radiation dose and reconstruction method. MBIR images obtained at 10 mA demonstrated significant decrease in numerator value for bar resolution pattern with 7 lp/cm. ASIR = adaptive statistical iterative reconstruction, FBP = filtered back projection, HU = Hounsfield unit

Korean Journal of Radiology
KJR

Subjective Findings from Patient Studies

Table 2 shows the overall confidence scores for the presence or absence of diffuse interstitial lung abnormalities on images generated using each of the different reconstruction methods. The average overall confidence scores ranged from 1.1 to 1.5 for LDCT images in the normal group. With respect to the abnormal group, the scores ranged from 5.1 to 8.7. Although there was a tendency of underestimation of the presence of interstitial lung disease by IR in the abnormal group, it was not statistically significant in each observer.

Despite the distortion of lesion perception described above, the overall confidence scores for the presence or absence of abnormalities were similar among the observers. The AUC values of confidence scores for the presence of abnormalities are shown in Supplementary Table 1 in the online-only Data Supplement. The mean AUC for HRCT with FBP was 0.978 and the mean AUC values for LDCT with FBP, ASIR, and MBIR reconstruction were 0.979, 0.972, and 0.963, respectively.

For images exhibiting diffuse interstitial lung abnormalities, the extent of disease was estimated by each radiologist (Table 3). When LDCT images (reconstructed with the FBP, ASIR, and MBIR methods) and standard dose HRCT images were compared, two of the four radiologists significantly overestimated the extent of ground glass opacity on the LDCT with FBP images. Three of the four radiologists significantly overestimated the extent of ground glass opacity on LDCT with ASIR and MBIR images. Overall, there was a trend of overestimation of ground glass opacity on FBP, ASIR, and MBIR images (+4.6%, +8.9%, and +8.5%, respectively), although the absolute percentages of the perceived types of abnormalities varied among the observers (Fig. 2). Figure 3 demonstrates examples of the smoothing effect in the ASIR and MBIR images compared with standard dose FBP images.

Among the four observers, two observers significantly underestimated the extent of reticular opacity or honeycombing lesions on FBP. The extent of reticular opacity or honeycombing was significantly underestimated by three observers on the ASIR images and by all four observers on the MBIR images (Table 3). The absolute percentage of perceived types of abnormalities varied among the observers; however, there was a trend of underestimation of reticular opacity or honeycombing on LDCT images reconstructed with FBP, ASIR, and MBIR (-2.8%, -4.1%, and -5.3%, respectively) compared to that on HRCT images (Fig. 2). There were no significant differences in the

Table 1. Results of Phantom Study: Numerator (NB[i]-NA[i]) Values (Unit: HU) According to Tube Current and Reconstruction Methods

lp/cm	10 mA						50 mA					
	FBP	ASIR 30%	ASIR 50%	ASIR 70%	ASIR 100%	MBIR	FBP	ASIR 30%	ASIR 50%	ASIR 70%	ASIR 100%	MBIR
4	1297	1330	1329	1289	1338	676	1155	1249	1301	1358	1424	1405
5	675	703	697	694	649	464	665	690	759	807	888	1180
6	272	196	198	145	150	536	364	251	265	256	250	1014
7	237	113	79	62	74	73	11	66	91	81	61	264

ASIR = adaptive statistical iterative reconstruction, FBP = filtered back projection, HU = Hounsfield unit, lp/cm = line pairs per centimeter, MBIR = model-based iterative reconstruction

Table 2. Results of Patient Study: Confidence Scores According to Readers for Presence of Abnormalities

	Reader A	*P*	Reader B	*P*	Reader C	*P*	Reader D	*P*
Normal group								
Series A	1.3		1.1		1.3		1.1	
Series B	1.5	0.22	1.3	1.00	1.1	0.06	1.1	0.09
Series C	1.4	0.15	1.3	0.01	1.3	0.84	1.1	0.00
Series D	1.4	0.40	1.3	0.02	1.4	0.50	1.2	0.00
Abnormal group								
Series A	8.8		5.8		8.6		6.3	
Series B	8.6	0.12	8.6	1.00	5.4	0.07	6.0	0.09
Series C	8.6	0.09	5.0	0.01	8.6	0.84	5.7	0.00
Series D	8.7	0.31	5.1	0.01	8.5	0.35	5.7	0.00

Series A = standard dose CT with FBP reconstruction, Series B = low-dose CT with FBP reconstruction, Series C = low-dose CT with ASIR reconstruction, Series D = low dose CT with MBIR reconstruction. ASIR = adaptive statistical iterative reconstruction, FBP = filtered back projection, MBIR = model-based iterative reconstruction

Table 3. Results of Patient Study: Average Percentage of Disease Extent According to Readers

	RET	*P*	GGO	*P*	CON	*P*
Reader A						
Series A	21.2		12.5		2.0	
Series B	20.1	0.38	15.2	0.07	2.8	0.06
Series C	20.5	0.59	17.5	0.00	2.5	0.24
Series D	17.6	0.01	13.0	0.69	2.6	0.10
Reader B						
Series A	17.0		9.9		1.7	
Series B	12.9	0.02	17.2	0.01	2.4	0.38
Series C	10.7	0.00	19.7	0.00	2.6	0.16
Series D	10.7	0.00	25.3	0.00	2.5	0.16
Reader C						
Series A	18.7		4.4		2.3	
Series B	15.4	0.04	5.5	0.40	2.0	0.56
Series C	14.9	0.01	4.6	0.84	2.2	0.84
Series D	13.1	0.00	6.1	0.10	1.8	0.47
Reader D						
Series A	19.6		9.4		1.4	
Series B	16.8	0.07	16.7	0.02	1.9	0.20
Series C	13.9	0.00	30.1	0.00	2.4	0.12
Series D	14.1	0.00	25.9	0.00	2.4	0.09

Series A = standard dose CT with FBP reconstruction, Series B = low-dose CT with FBP reconstruction, Series C = low dose CT with ASIR reconstruction, Series D = low-dose CT with MBIR reconstruction. ASIR = adaptive statistical iterative reconstruction, CON = consolidation, FBP = filtered back projection, GGO = ground glass opacity, MBIR = model-based iterative reconstruction, RET = reticular opacity or honeycombing

estimated extent of consolidation on HRCT images versus LDCT images using different methods of reconstruction.

With respect to the effect of three reconstruction methods in diagnosing DILD (UIP vs. NSIP or COP), Supplementary Table 2 in the online-only Data Supplement shows the AUCs for the overall confidence scores in the differentiation between UIP versus NSIP or COP (disease categorization). The mean AUC value for HRCT with FBP was 0.780 and the mean AUC values for LDCT reconstructed with FBP, ASIR, and MBIR in diagnosing UIP versus NSIP were 0.804, 0.785, and 0.778, respectively.

Radiation Doses

Supplementary Table 3 in the online-only Data Supplement shows $CTDI_{vol}$ and DLP for matched standard-dose HRCT and LDCT. While HRCT was a non-helical CT scan, LDCT scanning was performed in a helical manner following the institutional CT protocol for DILD evaluation. Despite this difference, the $CTDI_{vol}$ and DLP of LDCT were not substantially larger than those of non-helical HRCT. The mean value of $CTDI_{vol}$ was 1.79 ± 0.46 (range: 1.18–2.56) in the HRCT group and 1.87 ± 0.01 (range: 1.86–1.88) in the LDCT group. The mean DLP was 51.02 ± 13.10 mGy.cm (range: 26.17–78.19) in the HRCT group and 64.21 ± 5.82 mGy.cm (range: 52.67–75.98) in the LDCT group. The effective dose (ED) was calculated from DLP and it was found to be 0.7 ± 0.2 mSv (15) for patients in this study. Although few institutions use the less than 0.5 mSv radiation dose protocol with up to date IR equipment, chest CT with a radiation dose of less than 1.5 mSv can be considered as LDCT in general.

DISCUSSION

The results of the current study can be summarized by the following main findings: 1) MBIR was sub-optimal for a phantom structure requiring higher spatial resolution at a very low dose; 2) the type of reconstruction method did not significantly change the ability of the observer to identify diffuse interstitial lung abnormalities; 3) IR had a significant effect on estimation of the extent of ground glass opacity and reticular opacity or honeycombing; 4) the overestimation or underestimation of these interstitial abnormalities did not affect the radiologic diagnosis in typical DILD cases.

The use of CT to diagnose, manage and monitor IIPs is increasing in clinical practice. As treatments for idiopathic pulmonary fibrosis such as nintedanib (21) and pirfenidone (22) have been approved recently, assessment of disease severity by CT is mandated in clinical trials. Volumetric LDCT is expected to be useful for this longitudinal monitoring of DILD by facilitating quantitative assessment (23, 24) and by allowing a more comprehensive assessment of DILD (25) compared to conventional HRCT scans with sequential scanning at 10-mm intervals which provide only a reduced number of sections. With the development of IR technique, it has become possible to perform a submillisievert-dose volumetric CT scan. However, there are some disadvantages of IR. One of these concerns is the increased demand for computational power, which may prolong reconstruction times (26). Another concern is a noise-free appearance that can produce artifactual oversmoothing in ASIR (27) or MBIR reconstructed images (28, 29). In addition to these disadvantages, the current study suggested the possible disadvantage of IR under a submillisievert-dose setting for a condition in which high spatial resolution is needed.

With respect to the effect of IR on spatial resolution,

Korean Journal of Radiology
KJR

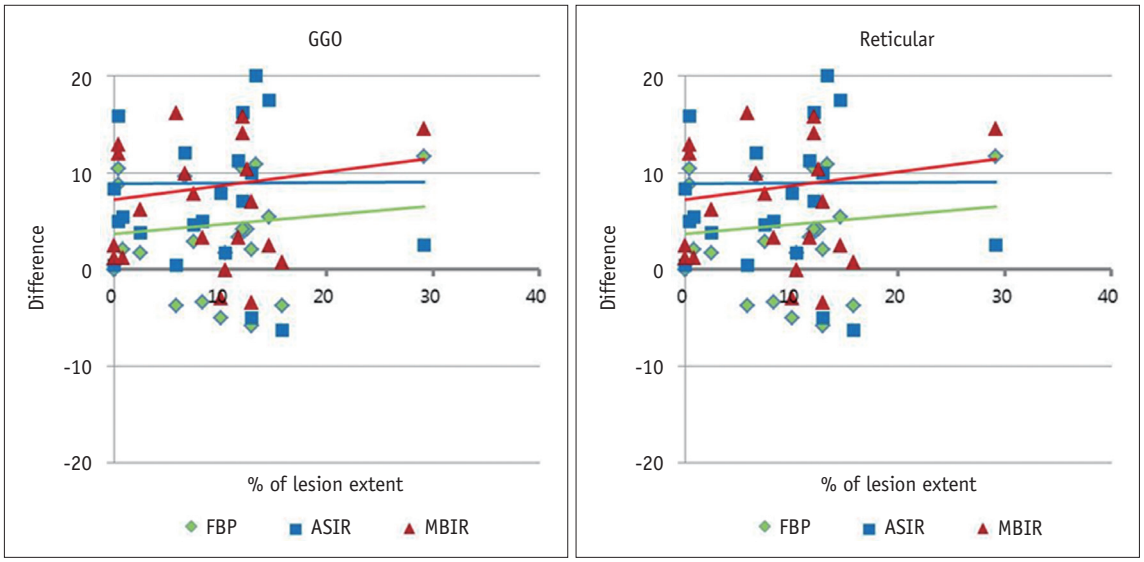

Fig. 2. Bland-Altman plots for each of four observers illustrating differences in measurement of disease extent based on FBP, ASIR, and MBIR images. With MBIR images, observers overestimated extent of GGO and underestimated extent of reticular opacity. However, there were no significant differences in evaluation of extent of consolidation (data not shown). ASIR = adaptive statistical iterative reconstruction, FBP = filtered back projection, GGO = ground glass opacity, MBIR = model-based iterative reconstruction

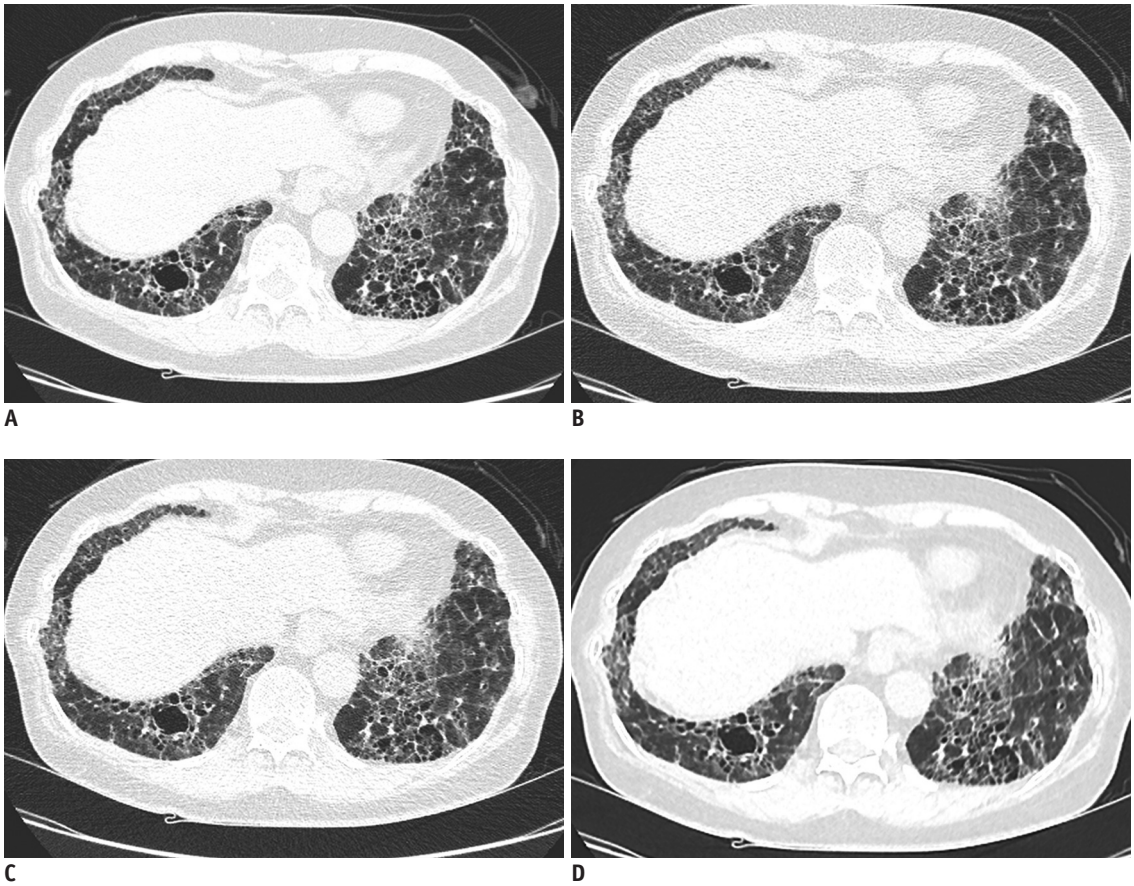

Fig. 3. Computed tomography (CT) images from a 69-year-old man with biopsy-proven usual interstitial pneumonia. **A.** Standard-dose HRCT image with FBP reconstruction. **B-D.** Exact same level images from raw data of low-dose CT reconstructed with **(B)** FBP, **(C)** ASIR, and **(D)** MBIR. Blurring phenomenon due to effect of MBIR, not due to respiratory artifact is shown in **(D)**. ASIR = adaptive statistical iterative reconstruction, FBP = filtered back projection, HRCT = high resolution computed tomography, MBIR = model-based iterative reconstruction

Ghetti et al. (30) previously performed a qualitative visual evaluation of high-resolution phantom images reconstructed with Iterative Reconstruction in Image Space (IRIS). They used the 120 kVp/200 mAs setting and reported that the IRIS images had a more blurry appearance compared with FBP images. Although there are previous patient studies reporting a pixelated blotchy appearance of MBIR (31, 32), our phantom study is the first study to demonstrate spatial resolution degradation in MBIR, especially under a condition requiring higher spatial resolution at a very low dose setting (120 kVp, 10 mA).

In our phantom study, MBIR resulted in a relatively lower numerator value at 10 mA and a relatively higher numerator value at 50 mA for the bar resolution patterns with 7 lp/cm when compared to the values provided by FBP. Also, there was a significant decrease in spatial resolution (i.e., steeper slope) of MBIR image between 6 lp/cm and 7 lp/cm at 10 mA. Therefore, it can be inferred that the spatial resolution is severely compromised in MBIR, a condition that requires higher spatial resolution at a very low dose. This finding was in contrast with that of previous research in which the authors reported that applications of MBIR algorithms greatly improve image quality by increasing resolution and reducing noise and artifacts (33). It is suggested that MBIR reduces image noise, but there is a point below which spatial resolution suffers. In our phantom study, that point existed between 6 lp/cm and 7 lp/cm when the phantom was scanned with 120 kVp and 10 mA or 50 mA. Although this point is not an absolute criterion for high spatial resolution, it can be inferred from our results that there may be reduced diagnostic quality of CT images from patients with DILD and that it cannot be improved with MBIR with regard to the conspicuity of relevant findings of fibrosis and interstitial lung disease. In our patient study, the mean ED of CT scans was well below the annual exposure to radiation from natural sources (3.1 mSv/year) and it was around 12 times greater than that delivered by chest posteroanterior- and lateral-projection radiographs (0.06 mSv for a standard patient) (34, 35). The radiation dose levels were similar between HRCT scans with sequential scanning at 10-mm intervals and volumetric LDCT scans. When we used standard-dose HRCT as the reference LDCT in our patient study, ASIR or MBIR reconstructed images showed similar diagnostic performance in typical cases for detection and diagnosis of DILD. The absolute percentage of perceived types of abnormalities varied among the observers, and it might be related to the difference in image appearance and lack of reader familiarity with IR images. This variability may decrease over the course of familiarization with IR images and further advancement in IR techniques. However, there clearly existed a greater trend of overestimation of ground glass opacity and underestimation of reticular opacity or honeycombing on LDCT images reconstructed with IR in our study. We should emphasize this blurring phenomenon of reticular opacity or honeycombing in LDCT using IR, which is partly in line with loss of spatial resolution proved by our phantom study. Therefore, caution is warranted when comparing disease extent, especially in follow-up studies reconstructed with IR, due to possible influence on the characterization of the interstitial lung disease pattern. In addition, further research will be helpful in dealing with diagnostic adequacy of low dose IR images for other lung abnormalities including those with low contrast.

There are several limitations to the present study. First, we could not calculate the real R(i) because the denominator values were not measured. However, the denominator values remain the same when we scan with a fixed radiation exposure and reconstruction method. Therefore, the comparison of the slope in our results (the decrease in the numerator value) could be a rational indirect way to demonstrate the compromised spatial resolution of MBIR in a situation in which high spatial resolution is required under very low radiation dose exposure. Second, since a surgical biopsy was not performed in all patients, only DILD patients with classical imaging findings were included. Third, ASIR with 50% blending was used in all patients irrespective of body weight. Due to the natural physical characteristics of the Asian population, the mean body mass index of patients in this study was relatively low. Fourth, the images acquired at the level of the aortic arch showed minimal abnormalities in some patients, which may have confounded the results. Finally, complete blinding was not possible because of the unique visual appearance of IR images despite the radiologists being blinded to the reconstruction methods. However, there was no way the readers could have known whether the images were reconstructed with ASIR or MBIR. It would also be interesting to investigate the impact of IR on the results of objective quantitative CT in DILD in the near future, which was not assessed in our study.

In conclusion, phantom images reconstructed with MBIR showed a potential to compromise spatial resolution in a very low dose setting. LDCT images reconstructed with

Korean Journal of Radiology
KJR

ASIR and MBIR in DILD patients resulted in overestimation of ground glass opacity and underestimation of reticular opacity or honeycombing by visual assessment. Although the diagnostic performance of LDCT with FBP, ASIR, and MBIR was similar to that of HRCT in typical DILD cases, caution should be exercised when comparing disease extent since the characterization of interstitial lung disease patterns can be influenced by IR reconstruction of follow-up imaging studies.

Supplementary Materials

The online-only Data Supplement is available with this article at https://doi.org/10.3348/kjr.2016.17.6.950.

REFERENCES

1. Kubo T, Lin PJ, Stiller W, Takahashi M, Kauczor HU, Ohno Y, et al. Radiation dose reduction in chest CT: a review. *AJR Am J Roentgenol* 2008;190:335-343
2. Mayo JR. CT evaluation of diffuse infiltrative lung disease: dose considerations and optimal technique. *J Thorac Imaging* 2009;24:252-259
3. Tsapaki V, Aldrich JE, Sharma R, Staniszewska MA, Krisanachinda A, Rehani M, et al. Dose reduction in CT while maintaining diagnostic confidence: diagnostic reference levels at routine head, chest, and abdominal CT--IAEA-coordinated research project. *Radiology* 2006;240:828-834
4. Kalra MK, Maher MM, Toth TL, Hamberg LM, Blake MA, Shepard JA, et al. Strategies for CT radiation dose optimization. *Radiology* 2004;230:619-628
5. Heyer CM, Mohr PS, Lemburg SP, Peters SA, Nicolas V. Image quality and radiation exposure at pulmonary CT angiography with 100- or 120-kVp protocol: prospective randomized study. *Radiology* 2007;245:577-583
6. Diel J, Perlmutter S, Venkataramanan N, Mueller R, Lane MJ, Katz DS. Unenhanced helical CT using increased pitch for suspected renal colic: an effective technique for radiation dose reduction?. *J Comput Assist Tomogr* 2000;24:795-801
7. Kalra MK, Maher MM, Sahani DV, Blake MA, Hahn PF, Avinash GB, et al. Low-dose CT of the abdomen: evaluation of image improvement with use of noise reduction filters pilot study. *Radiology* 2003;228:251-256
8. Thibault JB, Sauer KD, Bouman CA, Hsieh J. A three-dimensional statistical approach to improved image quality for multislice helical CT. *Med Phys* 2007;34:4526-4544
9. Machida H, Tanaka I, Fukui R, Kita K, Shen Y, Ueno E, et al. Improved delineation of the anterior spinal artery with model-based iterative reconstruction in CT angiography: a clinical pilot study. *AJR Am J Roentgenol* 2013;200:442-446
10. Shuman WP, Green DE, Busey JM, Kolokythas O, Mitsumori LM, Koprowicz KM, et al. Model-based iterative reconstruction versus adaptive statistical iterative reconstruction and filtered back projection in liver 64-MDCT: focal lesion detection, lesion conspicuity, and image noise. *AJR Am J Roentgenol* 2013;200:1071-1076
11. Goldman LW. Principles of CT: radiation dose and image quality. *J Nucl Med Technol* 2007;35:213-225; quiz 226-228
12. Goldman LW. Principles of CT and CT technology. *J Nucl Med Technol* 2007;35:115-128; quiz 129-130
13. Ichikawa Y, Kitagawa K, Nagasawa N, Murashima S, Sakuma H. CT of the chest with model-based, fully iterative reconstruction: comparison with adaptive statistical iterative reconstruction. *BMC Med Imaging* 2013;13:27
14. Pontana F, Billard AS, Duhamel A, Schmidt B, Faivre JB, Hachulla E, et al. Effect of iterative reconstruction on the detection of systemic sclerosis-related interstitial lung disease: clinical experience in 55 patients. *Radiology* 2016;279:297-305
15. AAPM. *The measurement, reporting, and management of radiation dose in CT*. Alexandria, VA: AAPM, 2008
16. Yoon HJ, Chung MJ, Hwang HS, Moon JW, Lee KS. Adaptive statistical iterative reconstruction-applied ultra-low-dose CT with radiography-comparable radiation dose: usefulness for lung nodule detection. *Korean J Radiol* 2015;16:1132-1141
17. Staude A, Goebbels J. *Determining the spatial resolution in computed tomography-comparison of MTF and line-pair structures*. International symposium on digital industrial radiology and computed tomography-Tu.4.1;2011 June 20-22;Berlin, Germany
18. Bland JM, Altman DG. Statistical methods for assessing agreement between two methods of clinical measurement. *Lancet* 1986;1:307-310
19. Dorfman DD, Berbaum KS, Metz CE. Receiver operating characteristic rating analysis. Generalization to the population of readers and patients with the jackknife method. *Invest Radiol* 1992;27:723-731
20. Obuchowski NA. New methodological tools for multiple-reader ROC studies. *Radiology* 2007;243:10-12
21. Richeldi L, du Bois RM, Raghu G, Azuma A, Brown KK, Costabel U, et al. Efficacy and safety of nintedanib in idiopathic pulmonary fibrosis. *N Engl J Med* 2014;370:2071-2082
22. King TE Jr, Bradford WZ, Castro-Bernardini S, Fagan EA, Glaspole I, Glassberg MK, et al. A phase 3 trial of pirfenidone in patients with idiopathic pulmonary fibrosis. *N Engl J Med* 2014;370:2083-2092
23. Sverzellati N, Zompatori M, De Luca G, Chetta A, Bnà C, Ormitti F, et al. Evaluation of quantitative CT indexes in idiopathic interstitial pneumonitis using a low-dose technique. *Eur J Radiol* 2005;56:370-375
24. Yabuuchi H, Matsuo Y, Tsukamoto H, Horiuchi T, Sunami S, Kamitani T, et al. Evaluation of the extent of ground-glass opacity on high-resolution CT in patients with interstitial pneumonia associated with systemic sclerosis: comparison between quantitative and qualitative analysis. *Clin Radiol* 2014;69:758-764

25. Bendaoud S, Remy-Jardin M, Wallaert B, Deken V, Duhamel A, Faivre JB, et al. Sequential versus volumetric computed tomography in the follow-up of chronic bronchopulmonary diseases: comparison of diagnostic information and radiation dose in 63 adults. *J Thorac Imaging* 2011;26:190-195
26. Xu J, Mahesh M, Tsui BM. Is iterative reconstruction ready for MDCT? *J Am Coll Radiol* 2009;6:274-276
27. Silva AC, Lawder HJ, Hara A, Kujak J, Pavlicek W. Innovations in CT dose reduction strategy: application of the adaptive statistical iterative reconstruction algorithm. *AJR Am J Roentgenol* 2010;194:191-199
28. Jiao de C, Li TF, Han XW, Wu G, Ma J, Fu MT, et al. Clinical applications of the C-arm cone-beam CT-based 3D needle guidance system in performing percutaneous transthoracic needle biopsy of pulmonary lesions. *Diagn Interv Radiol* 2014;20:470-474
29. Smith EA, Dillman JR, Goodsitt MM, Christodoulou EG, Keshavarzi N, Strouse PJ. Model-based iterative reconstruction: effect on patient radiation dose and image quality in pediatric body CT. *Radiology* 2014;270:526-534
30. Ghetti C, Ortenzia O, Serreli G. CT iterative reconstruction in image space: a phantom study. *Phys Med* 2012;28:161-165
31. Yamada Y, Jinzaki M, Tanami Y, Shiomi E, Sugiura H, Abe T, et al. Model-based iterative reconstruction technique for ultralow-dose computed tomography of the lung: a pilot study. *Invest Radiol* 2012;47:482-489
32. Katsura M, Matsuda I, Akahane M, Sato J, Akai H, Yasaka K, et al. Model-based iterative reconstruction technique for radiation dose reduction in chest CT: comparison with the adaptive statistical iterative reconstruction technique. *Eur Radiol* 2012;22:1613-1623
33. Yu Z, Thibault JB, Bouman CA, Sauer KD, Hsieh J. Fast model-based X-ray CT reconstruction using spatially nonhomogeneous ICD optimization. *IEEE Trans Image Process* 2011;20:161-175
34. McCollough CH, Chen GH, Kalender W, Leng S, Samei E, Taguchi K, et al. Achieving routine submillisievert CT scanning: report from the summit on management of radiation dose in CT. *Radiology* 2012;264:567-580
35. Wall BF, Hart D. Revised radiation doses for typical X-ray examinations. Report on a recent review of doses to patients from medical X-ray examinations in the UK by NRPB. National Radiological Protection Board. *Br J Radiol* 1997;70:437-439